Cao et al.
Chinese Journal of Mechanical Engineering (2022) 35:75
https://doi.org/10.1186/s10033-022-00756-7

Chinese Journal of Mechanical Engineering

ORIGINAL ARTICLE

Open Access

Efficient Inverse Method for Structural Identification Considering Modeling and Response Uncertainties

Lixiong Cao, Jie Liu*, Cheng Lu and Wei Wang

Abstract
The inverse problem analysis method provides an effective way for the structural parameter identification. However, uncertainties wildly exist in the practical engineering inverse problems. Due to the coupling of multi-source uncertainties in the measured responses and the modeling parameters, the traditional inverse method under the deterministic framework faces the challenges in solving mechanism and computing cost. In this paper, an uncertain inverse method based on convex model and dimension reduction decomposition is proposed to realize the interval identification of unknown structural parameters according to the uncertain measured responses and modeling parameters. Firstly, the polygonal convex set model is established to quantify the epistemic uncertainties of modeling parameters. Afterwards, a space collocation method based on dimension reduction decomposition is proposed to transform the inverse problem considering multi-source uncertainties into a few interval inverse problems considering response uncertainty. The transformed interval inverse problem involves the two-layer solving process including interval propagation and optimization updating. In order to solve the interval inverse problems considering response uncertainty, an efficient interval inverse method based on the high dimensional model representation and affine algorithm is further developed. Through the coupling of the above two strategies, the proposed uncertain inverse method avoids the time-consuming multi-layer nested calculation procedure, and then effectively realizes the uncertainty identification of unknown structural parameters. Finally, two engineering examples are provided to verify the effectiveness of the proposed uncertain inverse method.

Keywords: Inverse problem, Uncertainty quantification, Dimension reduction decomposition, Polygonal convex set, Affine algorithm

1 Introduction

Engineering problems are generally classified into the forward problems and the inverse problems. The forward problems aim at estimating the performance responses under the given physical system and external conditions, which are the analysis process. In contrast, the inverse problems are the comprehensive process of inferring internal parameters or external excitations from the testing or expected performances [1, 2]. Nowadays, the inverse problem analysis methods have received continuous attention from academia, and have been successfully applied in many engineering fields, such as the parameters estimation [3], the damage identification [4], the health monitoring [5] and the load identification [6], etc.

Actually, due to fluctuation of environment, randomness of material, measuring and manufacturing errors, and so on, uncertainties wildly exist in the practical engineering inverse problems [7–9]. However, the computational inverse methods under the deterministic framework have no ability to identify the influence of these uncertainties on the inverse results. Therefore, it

*Correspondence: liujie@hnu.edu.cn
State Key Laboratory of Advanced Design and Manufacturing for Vehicle Body, College of Mechanical and Vehicle Engineering, Hunan University, Changsha 410082, China

is very necessary to deeply study the uncertain inverse method to effectively evaluate these uncertainties and their effects on the inverse parameters. As shown in Figure 1, according to the location of uncertainty in the system function, uncertain inverse problems are divided into three categories: ① the inverse problem considering response uncertainty (IP-RU); ② the inverse problem considering modeling uncertainty (IP-MU); ③ the inverse problem considering modeling and response uncertainties (IP-MRU) that uncertainties exist in both the measured responses and some modeling parameters. Because the coupling of uncertainty analysis and inverse calculation, the solving of uncertain inverse problem often faces the bottleneck of complex nesting and large-scale computing.

The IP-RU aims to identify the unknown structural parameters under the deterministic system model and the uncertain measured responses. As the most widely used uncertainty quantification method, probability theory can effectively measure the uncertainty in measured responses [10–12]. So far, the researches about the IP-RU is relatively sufficient, and many advanced inverse methods are developed, mainly including the maximum likelihood estimation [13], the Bayesian inverse method [14], and the uncertainty propagation-based inverse method [15]. The maximum likelihood estimation and Bayesian approach commonly involve the random sampling process, the computational cost is expensive in practical engineering application [16, 17]. In recent years, the computational inverse method embedded uncertainty propagation has attracted extensive attention of scholars. The core of this kind of inverse method is to build the uncertainty optimization matching model of the measured and calculated responses for inversing the unknown parameters [18]. In the IP-MU, some system modeling parameters are uncertain, and the measured responses are deterministic. Generally, it is necessary to conduct the uncertain sampling for modeling parameters, and then estimate the influence of the uncertainties on the identified parameters according to the deterministic inverse results under each sampling point [19, 20]. Compared with the IP-RU, the researches about IP-MU are relatively few at present.

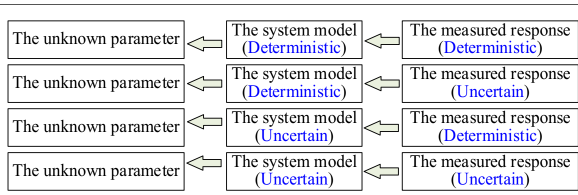

Figure 1 Classification of uncertain inverse problems

Generally, uncertainties are classified into stochastic uncertainty and epistemic uncertainty. Stochastic uncertainty is derived from the inherent randomness of system or environment, which is usually described by the probabilistic model [21, 22]. Epistemic uncertainty is often caused by incompleteness of knowledge to some extent [23, 24]. However, the probabilistic model is based on the sufficient sample information and the explicit probability distribution type. Unfortunately, only the limited data is available in the practical engineering problems because of constrains of economic and technical conditions. Therefore, it is difficult to construct a complete probability distribution according to the incomplete knowledge and data. The non-probabilistic convex model method can evaluate the boundaries of uncertain parameters with the limited sample data, and provide an alternative way for quantitative representation of epistemic uncertainties. The typical convex model includes interval model [25], ellipsoid model [26], parallelepiped model [27] and polygonal convex set (PCS) model [28]. At present, the interval model has been applied to the practical engineering inverse problems because of its convenience. For the IP-RU, Faes et al. [29] proposed an effective multivariate interval method to inversely assess the uncertainty of parameter under limited experimental data. Jiang et al. [30] realized the uncertainty identification of material parameters for composite laminates by constructing the interval error optimization model. For the IP-MU, Liu et al. [31] developed a dynamic load identification method based on Gegenbauer polynomial and regularization method to evaluate the influence of system uncertainty on the identified load. Xu et al. [32] proposed a sequential two-stage interval identification method based on Tikhonov regularization, and achieved the interval identification of dynamic load under the uncertain structure.

In practical engineering inverse problems, due to the changeable working conditions, the complex multi physical processes and the measuring and processing errors, uncertainties often exist in the model itself and the measured responses at the same time. In fact, this kind of IP-MRU is more common in practical engineering problems. However, because of the coupling of these multi-source uncertainties, the solving for this kind of uncertain inverse problem involves the complex multi-layer nesting. In view of that, it is difficult to investigate the inverse propagation mechanism of uncertainties in engineering structures, and then it is also impossible to realize the solving of this kind of uncertain inverse problem and uncertainty quantification of the unknown parameters. At present, the researches about IP-MRU are in the exploration stage, there are few reports about the effective solving method. Therefore, it has the great practical significance to study the efficient uncertain inverse method for the parameter identification and high-precision modeling in engineering problems.

In this paper, a general solving framework based on convex model for IP-MRU is presented, and an efficient uncertain inverse method is further proposed to realize the inverse uncertainty identification of unknown structural parameters. The remainder of this paper is organized as follows. In Section 2, the inverse problem considering multi-source uncertainties is descripted, and a basic solving framework is presented. In Section 3, the efficient uncertain method is presented in detailed. In the proposed method, the PCS model and the interval model are employed to quantify uncertainties in the modeling parameters and the measured responses respectively, and an uncertain inverse method based on dimension reduction decomposition (DRD) is developed to realize the solving of IP-MRU. Two examples are provided to show the effectiveness of the proposed uncertain inverse method in Section 4. The conclusions of this paper are summarized in Section 5.

2 Description of IP-MRU

The effective forward model is the premise and foundation for solving the inverse problem. For IP-MRU, the forward structure model $\boldsymbol{G}$ is generally expressed as

$$\begin{cases} \boldsymbol{Y} = \boldsymbol{G}(\boldsymbol{X}, \boldsymbol{U}), \\ Y_i = G_i(X_1, X_2, \cdots, X_m, U_1, U_2, \cdots, U_n), \\ i = 1, 2, \cdots, p, \end{cases} \tag{1}$$

where $\boldsymbol{Y}$ is the p-dimensional vector of structural responses, $\boldsymbol{U}$ is the n-dimensional vector of the known but uncertain modeling parameters, and $\boldsymbol{X}$ is the m-dimensional unknown modeling or input parameters that need to be identified. In order to distinguish them effectively, the known and uncertain structural modeling parameters are called "uncertain variables", and the unknown structural modeling parameters that need to be identified are called "unknown parameters". Generally, the dimension p of $\boldsymbol{Y}$ is greater than or equal to the dimension m of $\boldsymbol{X}$, so that the inverse problem has the positive definite solution. Due to the lack of testing data and the limitation of physical knowledge, the responses $\boldsymbol{Y}$ and variables $\boldsymbol{U}$ are uncertain. The purpose of this kind of uncertain inverse problem is to identify unknown parameters $\boldsymbol{X}$ and their uncertainties according to the uncertain responses and system model. In view of that, the IP-MRU can be descripted as

$$\begin{cases} F : f_{\boldsymbol{X}}(\boldsymbol{X}) \leftarrow \left\{ f_{\boldsymbol{U}}(\boldsymbol{U}), f_{\boldsymbol{Y}}(\boldsymbol{Y}) \right\}, \\ \text{s.t.} \boldsymbol{Y} = \boldsymbol{G}(\boldsymbol{X}, \boldsymbol{U}), \end{cases} \tag{2}$$

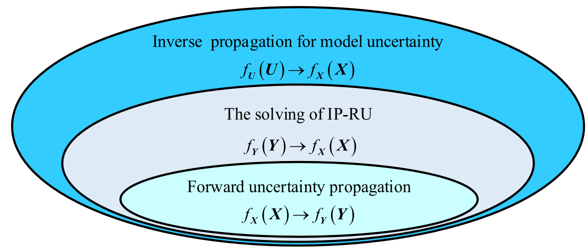

Figure 2 The basic solving framework for IP-MRU

where $f_{\boldsymbol{U}}$, $f_{\boldsymbol{Y}}$ and $f_{\boldsymbol{X}}$ denote the uncertainty measurement for the responses $\boldsymbol{Y}$, the variables $\boldsymbol{U}$ and the unknown parameters $\boldsymbol{X}$, respectively. In this study, the measured responses $\boldsymbol{Y}$ are modeled by the interval model, namely, the left and right boundaries are known, and the uncertain structural variables $\boldsymbol{U}$ are quantified by PCS model. F represents the mapping relation of the uncertainties from the responses $\boldsymbol{Y}$ and variables $\boldsymbol{U}$ to the unknown parameters $\boldsymbol{X}$. It can be found from Eq. (2) that the IP-MRU is actually an inverse uncertainty propagation process under the constraint of forward structure model. For the convenience of expression, the IP-MRU described in Eq. (2) can be expressed as

$$\begin{cases} \boldsymbol{X} = \overleftarrow{\boldsymbol{G}}(\boldsymbol{U}, \boldsymbol{Y}), X_i = \overleftarrow{G_i}(\boldsymbol{U}, \boldsymbol{Y}), i = 1, 2, \cdots, m, \\ \text{s.t.} \boldsymbol{U} \in f_{\boldsymbol{U}}(\boldsymbol{U}), \boldsymbol{Y} \in f_{\boldsymbol{Y}}(\boldsymbol{Y}), \end{cases} \tag{3}$$

where $\overleftarrow{G_i}$ denotes the inverse function of X_i with respect to the responses $\boldsymbol{Y}$ and variables $\boldsymbol{U}$. All inverse functions $\overleftarrow{G_i}$ constitute the system inverse function $\overleftarrow{\boldsymbol{G}}$. Through the inverse uncertainty propagation, the left and right boundaries of unknown parameters $\boldsymbol{X}$ can be identified.

Due to the coupling of the response uncertainty and the modeling uncertainty, it is difficult to explore the inverse propagation mechanism of response and modeling uncertainties. The basic idea for solving this kind of uncertain inverse problem is to decouple the response uncertainty and modeling uncertainty in the inverse problem, and then transform the IP-MRU into the inverse problem with single-source uncertainty. Actually, if a set of specific values of uncertain modeling variables $\boldsymbol{U}$ are given, the structure model will be deterministic. Under these circumstances, the IP-MRU in Eq. (2) can degenerate into an IP-RU. For the IP-RU, the uncertainty propagation-based inverse method can be employed to inverse the intervals of unknown parameters. In which, the out layer is the interval matching optimization of the measured and calculated responses, and the inner layer is the interval propagation analysis process. On the basis of the above statement, a basic solving framework involving multi-layer nesting for the IP-MRU are presented as shown in Figure 2:

(1) The outer layer is the inverse uncertainty propagation process for modeling uncertainty. Through Monte Carlo Simulation (MCS) in the convex model of variables $\boldsymbol{U}$, the IP-MRU is transformed into a series of IP-RU under each sampling point.
(2) The middle layer is the solving of IP-RU under the deterministic variables $\boldsymbol{U}$. Solving the interval optimization matching model of the measured and calculated responses, the left and right boundaries of unknown parameters $\boldsymbol{X}$ can be obtained.
(3) The inner layer is the forward uncertainty propagation process to obtain the calculated responses in the middle layer. Through the interval propagation analysis, the intervals of responses $\boldsymbol{Y}$ can be calculated according to the given intervals of unknown parameters $\boldsymbol{X}$.

According to the above inverse calculation, the intervals for the unknown parameters $\boldsymbol{X}$ will be obtained under each sampling point of uncertain variables $\boldsymbol{U}$. Thus, the final left and right boundaries of unknown parameters $\boldsymbol{X}$ can be identified through the statistical comparison of all inverse results. It can be found that the solving of IP-MRU is a multi-layer nested complex calculation process. Involving MCS, optimization and uncertainty propagation, the whole inverse process faces the bottleneck problem of large-scale computation.

3 Uncertain Inverse Method Based on PCS Model and DRD

From the above discussion, it can be obviously seen that the uncertain inverse problem as shown in Eq. (2) faces the unbearable computational cost due to the multi-layer nesting solving process. In this section, an effective uncertain inverse method based on PCS and DRD is proposed to realize the inverse uncertainty identification of unknown parameters. Firstly, PCS is employed to quantify the uncertainties and correlation of variables $\boldsymbol{U}$ according to the limited sample information. Secondly, an efficient space collocation method based on DRD is proposed to transform the IP-MRU into a few IP-RU. Finally, an interval inverse method based on high dimensional model representation (HDMR) and affine algorithm is further presented to effectively solve the IP-RU.

3.1 PCS Model for Quantifying Modeling Uncertainty

In practical engineering problems, the sample distributions of uncertain modeling variables are usually complex and various, and there is a certain correlation. Compared with the traditional convex model with the simple regular shape, PCS model provides a more suitable and reasonable way to quantify uncertainty and correlation with limited sample information by using the irregular boundaries.

Assuming that there are N experimental samples $\boldsymbol{U}^N=\left[\boldsymbol{U}^{(1)},\boldsymbol{U}^{(2)},\cdots,\boldsymbol{U}^{(N)}\right]$ of n-dimensional uncertain modeling variables $\boldsymbol{U}$, where $\boldsymbol{U}^{(N)}=\left[U_1^{(N)},U_2^{(N)},\cdots,U_n^{(N)}\right]^{\mathrm{T}}$. According to the samples, a traditional interval model is firstly established, which is expressed as

$$\Omega_{\mathrm{I}}=\left\{\boldsymbol{U}|\boldsymbol{U}^{\mathrm{L}}\leq\boldsymbol{U}\leq\boldsymbol{U}^{\mathrm{R}}\right\},\tag{4}$$

where $\boldsymbol{U}^{\mathrm{L}}=\min\left(\boldsymbol{U}^N\right)$ and $\boldsymbol{U}^{\mathrm{R}}=\max\left(\boldsymbol{U}^N\right)$ represent the left and right boundaries of variables $\boldsymbol{U}$; Ω_{I} denotes the uncertainty domain of interval model. In order to reasonably quantify the correlation in sample data, a principal component analysis (PCA) interval model will be further established. For the known samples $\boldsymbol{U}^N$, the mean point can be calculated as

$$\boldsymbol{U}^{\mathrm{M}}=\frac{1}{N}\left[\sum_{t=1}^{N}U_1^{(t)},\sum_{t=1}^{N}U_2^{(t)},\cdots,\sum_{t=1}^{N}U_n^{(t)}\right]^{\mathrm{T}}.\tag{5}$$

The covariance matrix $\boldsymbol{C}$ for uncertain samples is defined as

$$\boldsymbol{C}=\frac{1}{n}\left(\boldsymbol{U}^N-\overline{\boldsymbol{U}}^{\mathrm{M}}\right)\left(\boldsymbol{U}^N-\overline{\boldsymbol{U}}^{\mathrm{M}}\right)^{\mathrm{T}},\tag{6}$$

where $\overline{\boldsymbol{U}}^{\mathrm{M}}=\left[\boldsymbol{U}^{\mathrm{M}},\boldsymbol{U}^{\mathrm{M}},\cdots,\boldsymbol{U}^{\mathrm{M}}\right]_{n\times N}$ is the mean matrix composed of N mean points $\boldsymbol{U}^{\mathrm{M}}$. Through PCA, the orthogonal eigenvectors with respect to the covariance matrix $\boldsymbol{p}_i=(p_{1i},p_{2i},\cdots,p_{ni})^{\mathrm{T}},i=1,2,\cdots,n$ can be obtained, which are rewritten as a matrix $\boldsymbol{P}=\left(\boldsymbol{p}_1,\boldsymbol{p}_2,\cdots,\boldsymbol{p}_n\right)$ by the decreasing order. Thus, a new coordinate system can be constructed based on these orthogonal eigenvector directions, and the uncertain modeling variables $\boldsymbol{U}$ and the samples $\boldsymbol{U}^N$ can be projected to the new coordinate system through matrix $\boldsymbol{P}$

$$\boldsymbol{Z}=\boldsymbol{P}^{\mathrm{T}}\left(\boldsymbol{U}-\boldsymbol{U}^{\mathrm{M}}\right).\tag{7}$$

In the new coordinate system, the correlation coefficient between any two of variables $\boldsymbol{Z}$ are zero. According to the transformed samples $\boldsymbol{Z}^N$, a new interval model based on PCA can be established as

$$\Omega_{\mathrm{IP}}=\left\{\boldsymbol{U}|\boldsymbol{Z}^{\mathrm{L}}\leq\boldsymbol{P}^{\mathrm{T}}\left(\boldsymbol{U}-\boldsymbol{U}^{\mathrm{M}}\right)\leq\boldsymbol{Z}^{\mathrm{R}}\right\},\tag{8}$$

where $\boldsymbol{Z}^{\mathrm{L}}=\min\left(\boldsymbol{Z}^N\right)$ and $\boldsymbol{Z}^{\mathrm{R}}=\max\left(\boldsymbol{Z}^N\right)$ represent the left and right boundaries of variables $\boldsymbol{Z}$. Ω_{IP} denotes the uncertainty domain of PCA interval model. In view

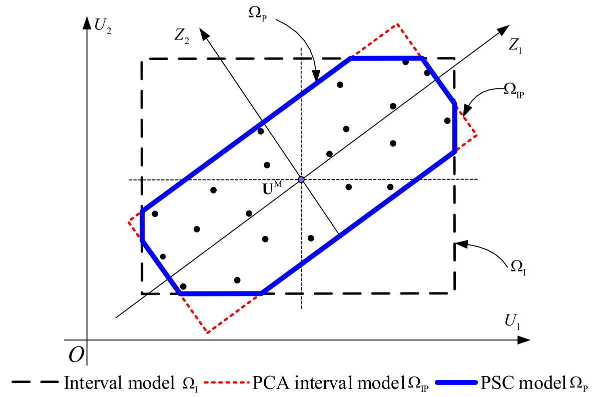

Figure 3 The two-dimensional PCS model

of that, the PCS model is established by combining the intersecting region between Ω_{I} and Ω_{IP}.

$$\Omega_{\mathrm{P}} = \left\{ \boldsymbol{U} | \boldsymbol{U}^{\mathrm{L}} \le \boldsymbol{U} \le \boldsymbol{U}^{\mathrm{R}} \cap \boldsymbol{Z}^{\mathrm{L}} \le \boldsymbol{P}^{\mathrm{T}} \left(\boldsymbol{U} - \boldsymbol{U}^{\mathrm{M}} \right) \le \boldsymbol{Z}^{\mathrm{R}} \right\}, \tag{9}$$

where Ω_{P} denotes the uncertainty domain of PCS model.

The examples of the two-dimensional PCS model is shown in Figure 3, it can be found that PCS model envelops all samples through the irregular minimum area. Therefore, the PCS model effectively quantifies the uncertainty represented by the given limited sample information. The more properties of PCS model can be seen in Ref. [28].

3.2 Space Collocation Method Based on DRD for Decoupling IP-MRU

As described in Section 2, MCS can realize the decoupling of response and modeling uncertainties, and then transform the IP-MRU into the IP-RU under each sampling point. However, the corresponding solving is unacceptable involving the random sampling. In this section, an efficient space collocation method based on DRD is proposed to replace MCS process, and then transforms the IP-MRU into a small amount IP-RU under collocation points (CPs).

The DRD method [33, 34] provides an efficient analysis framework for uncertainty propagation. This method effectively relieves the computational complexity of uncertainty propagation through transforming the structural performance function into the linear combination of univariate sub functions. Similarly, through the DRD for uncertain modeling variables $\boldsymbol{U}$, the inverse function $\overleftarrow{G}$ can be represented as

$$\boldsymbol{X} = \overleftarrow{\boldsymbol{G}}(\boldsymbol{U}, \boldsymbol{Y}) \simeq \sum_{i=1}^{n} \overleftarrow{\boldsymbol{G}}_i(\boldsymbol{U}_{-i}, \boldsymbol{Y}) - (n-1)\overleftarrow{\boldsymbol{G}}\left(\boldsymbol{U}^{\mathrm{C}}, \boldsymbol{Y}\right), \tag{10}$$

$$\overleftarrow{\boldsymbol{G}}_i(\boldsymbol{U}_{-i}, \boldsymbol{Y}) = \overleftarrow{\boldsymbol{G}}\left(U_1^{\mathrm{C}}, \cdots, U_{i-1}^{\mathrm{C}}, U_i, U_{i+1}^{\mathrm{C}}, \cdots, U_n^{\mathrm{C}}, \boldsymbol{Y}\right), \tag{11}$$

where $\boldsymbol{U}^{\mathrm{C}}$ denotes the decomposition midpoint of function.

It can be found from Eq. (10) that the responses of inverse function can be efficiently predicted through the linear combination of the responses of each sub inverse function. In this paper, the mean point of PCS model is selected to conduct DRD, namely, $\boldsymbol{U}^{\mathrm{C}} = \boldsymbol{U}^{\mathrm{M}}$. Figure 4 is schematic diagram of DRD for 3-dimensional problem. Assuming that k_i marginal CPs are taken for the sub inverse function $\overleftarrow{\boldsymbol{G}}_i$, and the l_ith marginal CP on the ith expansion axis is $\boldsymbol{U}_{-i}^{l_i} = \left[U_1^{\mathrm{M}}, \cdots, U_{i-1}^{\mathrm{M}}, U_i^{l_i}, U_{i+1}^{\mathrm{M}}, \cdots, U_n^{\mathrm{M}}\right]$. Because the measured responses are intervals $\boldsymbol{Y}^{\mathrm{I}}$, the solving of sub inverse function under the marginal CP $\boldsymbol{U}_{-i}^{i_k}$ is an interval-based IP-RU. For the convenience of expression, the corresponding IP-RU is expressed as

$$\begin{aligned} \boldsymbol{X}_i^{\mathrm{I}}(l_i) &= \overleftarrow{\boldsymbol{G}}_i\left(\boldsymbol{U}_{-i}^{l_i}, \boldsymbol{Y}^{\mathrm{I}}\right) \\ &= \overleftarrow{\boldsymbol{G}}\left(U_1^{\mathrm{M}}, \cdots, U_{i-1}^{\mathrm{M}}, U_{-i}^{l_i}, U_{i+1}^{\mathrm{M}}, \cdots, U_n^{\mathrm{M}}, \boldsymbol{Y}^{\mathrm{I}}\right), \end{aligned} \tag{12}$$

where $i = 1, 2, \cdots, m$, and $l_i = 1, 2, \cdots, k_i$.

The solving of IP-RU will be discussed in detail in Section 3.3. Here, it only needs to understand that the intervals of unknown parameter $\boldsymbol{X}$ can be obtained through Eq. (12). Because the inverse function is the linear combination of univariate sub inverse functions, the response intervals of

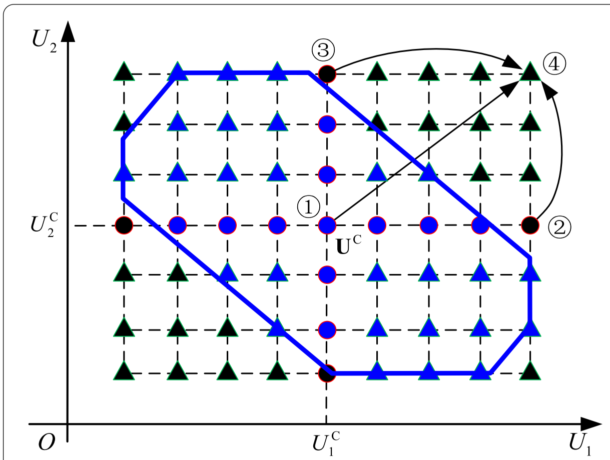

Figure 4 The schematic diagram of space collocation method

inverse function $\boldsymbol{X}^{\mathrm{I}}$ at any joint CP $\left[U_1^{l_1},\cdots,U_i^{l_i},\cdots,U_n^{l_n}\right]$ marked with triangle can be efficiently predicted through the linear combination of the response intervals of sub inverse function corresponding to marginal CPs marked with dot.

$$\begin{aligned}\boldsymbol{X}^{\mathrm{I}}(l_1,\cdots l_i,\cdots,l_n) &= \overleftarrow{\boldsymbol{G}}\left(U_1^{l_1},\cdots,U_i^{l_i},\cdots,U_n^{l_n},\overline{\boldsymbol{Y}}^{\mathrm{I}}\right)\\ &\simeq \sum_{i=1}^{n}\overleftarrow{\boldsymbol{G}}_i\left(\boldsymbol{U}_{-i}^{l_i},\overline{\boldsymbol{Y}}^{\mathrm{I}}\right)-(n-1)\overleftarrow{\boldsymbol{G}}\left(\boldsymbol{U}^{\mathrm{M}},\overline{\boldsymbol{Y}}^{\mathrm{I}}\right)\\ &= \sum_{i=1}^{n}\boldsymbol{X}_{\mathrm{i}}^{\mathrm{I}}(l_i)-K^{\mathrm{I}}.\end{aligned} \tag{13}$$

In order to ensure the propagation of correlation, it is necessary to ensure that all CPs are located in the uncertainty domain of PCS model, which can be easily realized by eliminating samples outside the uncertainty domain using Eq. (9). As shown in Figure 4, by comparing the all inverse intervals of IP-RU corresponding to the CPs marked with blue in the PCS model, the intervals of unknown parameters $\boldsymbol{X}$ with respect to the IP-MRU can be effectively obtained.

In summary, the proposed space collocation method based on DRD realizes the efficient decoupling of IP-MRU, and transforms the IP-MRU into a small number of IP-RU under marginal CPs. Compared with MCS, the proposed method effectively avoids the solving of a large number of IP-RU under random samples, and relieves the complexity and efficiency of solving calculation.

3.3 Interval Inverse Method Based on Affine Algorithm for IP-RU

Through the above discussion, it can be known that the IP-MRU is transformed into a small number of IP-RU under marginal CPs of variables $\boldsymbol{U}$. In this paper, the uncertainty propagation-based inverse method is adopted to realize the solving of IP-RU under each marginal CP.

Assuming that $\mathbf{U}^{\mathrm{P}}$ is a known marginal CP, the corresponding IP-RU can be expressed as

$$\begin{aligned}&\boldsymbol{X}=\overleftarrow{\boldsymbol{G}}\left(\boldsymbol{U}^{\mathrm{P}},\boldsymbol{Y}\right),X_i=\overleftarrow{G}_i\left(\boldsymbol{U}^{\mathrm{P}},\boldsymbol{Y}\right),i=1,2,\cdots,m,\\ &\text{s.t.}\boldsymbol{Y}\in\overline{\boldsymbol{Y}}^{\mathrm{I}}.\end{aligned} \tag{14}$$

Through establishing the interval matching model of the measured and calculated responses, this kind of IP-RU can be effectively solved [35].

$$\min\left\|\boldsymbol{Y}^{\mathrm{I}}\left(\boldsymbol{X}^{\mathrm{L}},\boldsymbol{X}^{\mathrm{R}}\right)-\overline{\boldsymbol{Y}}^{\mathrm{I}}\right\|, \tag{15}$$

where $\boldsymbol{X}^{\mathrm{L}}=\left[X_1^{\mathrm{L}},X_2^{\mathrm{L}},\cdots,X_m^{\mathrm{L}}\right]$ and $\boldsymbol{X}^{\mathrm{R}}=\left[X_1^{\mathrm{R}},X_2^{\mathrm{R}},\cdots,X_m^{\mathrm{R}}\right]$ are the left and right boundary vectors of unknown parameters, which are the variables to be inversed. $\boldsymbol{Y}^{\mathrm{I}}$ denotes the interval vector of calculated responses corresponding to the given $\boldsymbol{X}^{\mathrm{L}}$ and $\boldsymbol{X}^{\mathrm{R}}$. In this paper, the genetic algorithm (GA) is adopted to solve this optimization model in Eq. (15). In out layer, $\boldsymbol{X}^{\mathrm{L}}$ and $\boldsymbol{X}^{\mathrm{R}}$ will be updated using GA. In inner layer, the $\boldsymbol{Y}^{\mathrm{I}}$ with respect to the given $\boldsymbol{X}^{\mathrm{L}}$ and $\boldsymbol{X}^{\mathrm{R}}$ is calculated by the interval propagation analysis.

Involving the interval propagation analysis in inner layer, the solving of Eq. (15) will consume a larger number of forward model. In order to obtain the calculated responses $\boldsymbol{Y}^{\mathrm{I}}$ effectively, the first-order high dimensional model representation (HDMR) of forward model is further expressed as

$$\boldsymbol{Y}=\boldsymbol{G}\left(\boldsymbol{X},\boldsymbol{U}^{\mathrm{P}}\right)\simeq\sum_{j=1}^{m}\boldsymbol{G}_j\left(\boldsymbol{X}_{-j},\boldsymbol{U}^{\mathrm{P}}\right)-(m-1)\boldsymbol{G}\left(\boldsymbol{X}^{\mathrm{C}},\boldsymbol{U}^{\mathrm{P}}\right), \tag{16}$$

$$\boldsymbol{G}_j\left(\boldsymbol{X}_{-j},\boldsymbol{U}^{\mathrm{P}}\right)=\boldsymbol{G}_j\left(X_1^{\mathrm{C}},\cdots,X_{j-1}^{C},X_j,X_{j+1}^{C},\cdots,X_m^{\mathrm{C}},\boldsymbol{U}^{\mathrm{P}}\right), \tag{17}$$

where $\boldsymbol{X}^{\mathrm{C}}=\left(\boldsymbol{X}^{\mathrm{L}}+\boldsymbol{X}^{\mathrm{R}}\right)/2$ is the decomposition midpoint of the forward model.

For the jth univariate sub function G_{ij} of the ith response Y_i, the polynomial-based response surface model is adopted to establish the corresponding surrogate model

$$G_{ij}\left(\boldsymbol{X}_{-j},\boldsymbol{U}^{\mathrm{P}}\right)=\sum_{s=0}^{h}a_{i(s)}X_j^s, \tag{18}$$

where h denotes the highest order of polynomial surrogate model, $a_{i(s)}$ is the coefficient of s-order sub term. The order number h is usually determined according to the nonlinear degree of system, while the 3-order is usually enough for the univariate sub function. In view of that, the polynomial surrogate model for univariate sub function can be easily established by taking a small number of samples. Due to the explicit polynomial model, the interval $\boldsymbol{X}^{\mathrm{I}}$ can be directly substituted into Eqs. (16) and (18) to obtain the interval Y_i^{I}. However, the calculation results have the interval expansion problem because of the interval operation. In order to the left and right boundaries of each sub function, the affine algorithm is employed to conduct the interval propagation.

Firstly, the variable X_j is rewritten by the affine form

$$\hat{X}_j = X_j^{\mathrm{C}} + \xi X_j^{\mathrm{W}}, \xi \in [-1, 1], \tag{19}$$

where $X_j^{\mathrm{C}} = \frac{X_j^{\mathrm{U}} + X_j^{\mathrm{L}}}{2}$, $X_j^{\mathrm{W}} = \frac{X_j^{\mathrm{U}} - X_j^{\mathrm{L}}}{2}$.

Substituting Eq. (19) into Eq. (18), the sub function can be expressed in Eq. (20) through the binomial theorem.

$$\begin{aligned} G_{ij}\left(\boldsymbol{X}_{-j}, \boldsymbol{U}^{\mathrm{P}}\right) &= \sum_{s=0}^{h} a_{j(s)} \left(X_j^{\mathrm{C}} + \xi X_j^{\mathrm{W}}\right)^s \\ &= \sum_{s=0}^{h} \sum_{t=s}^{h} a_{j(t)} \binom{t}{s} \left(X_j^{\mathrm{C}}\right)^{t-s} \left(X_j^{\mathrm{W}}\right)^s \xi^s. \end{aligned} \tag{20}$$

Because $\xi \in [-1, 1]$, if s is even, $\xi^s \in [0, 1]$, if s is odd, $\xi^s \in [-1, 1]$. Thus, the interval expansion problem is avoided effectively. Under these circumstances, the interval [-1, 1] can be directly substituted into Eq. (20) to obtain the left and right boundary vectors of sub function G_{ij}. For the convenience of expression, there is

$$b_{j(t)} = \sum_{t=s}^{h} a_{j(t)} \binom{t}{s} \left(X_j^{C}\right)^{t-s} \left(X_j^{W}\right)^s. \tag{21}$$

The left and right boundary vectors of sub function G_{ij} can be expressed as

$$\begin{cases} G_{ij}^{\mathrm{R}}\left(\boldsymbol{X}_{-j}, \boldsymbol{U}^{\mathrm{P}}\right) = b_{j(0)} + \sum\limits_{s=1}^{h} \begin{cases} \max\left(0, b_{j(s)}\right) s = 2A, \\ \left|b_{j(s)}\right| s = 2A + 1, \end{cases} \\ G_{ij}^{\mathrm{L}}\left(\boldsymbol{X}_{-j}, \boldsymbol{U}^{\mathrm{P}}\right) = b_{j(0)} + \sum\limits_{s=1}^{h} \begin{cases} \min\left(0, b_{j(s)}\right) s = 2A, \\ -\left|b_{j(s)}\right| s = 2A + 1, \end{cases} \end{cases} \tag{22}$$

where A denotes arbitrary integer. Similar with Eq. (13), substituting Eq. (22) into Eq. (13), the intervals $\boldsymbol{Y}^{\mathrm{I}}$ can be calculated.

Overall, the above interval inverse method based on HDMR and affine algorithm efficiently improves the inverse efficiency IP-RU, which can obtain the left and right boundaries of unknown parameter $\boldsymbol{X}$ only calling a few forward problem functions. In view of that, the intervals $\boldsymbol{X}^{\mathrm{I}}$ under each marginal CP all can be effectively obtained.

3.4 Solving Procedure

To summarize, the solving process of the proposed uncertain method can be divided into three parts. The first part is the uncertainty modeling for the variables $\boldsymbol{U}$ and the measured responses $\boldsymbol{Y}$, in which the variables $\boldsymbol{U}$ are quantified by PCS model, the measured responses $\boldsymbol{Y}$ are modeled by the interval model. The second part is the decoupling of IP-MRU, the complex nesting solving process is transformed into a small

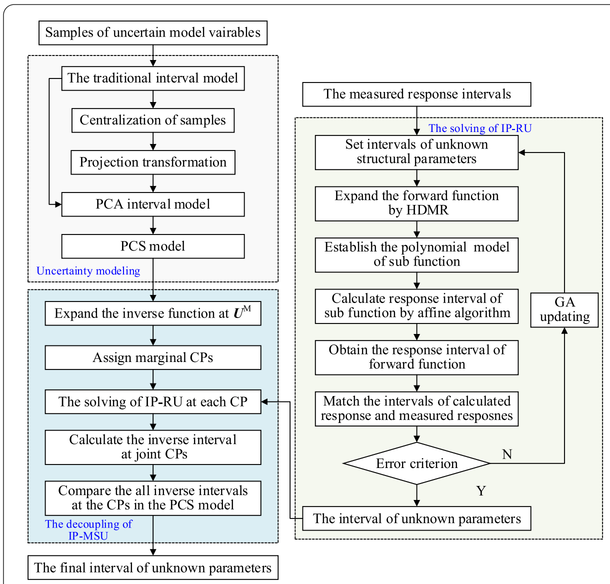

Figure 5 The inverse flowchart of IP-MRU

amount of IP-RU calculation through the proposed space collocation method based DRD. The third part is the solving of IP-RU under CPs, in which the inverse efficiency is efficiently improved through affine algorithm and HDMR based on the polynomial response surface. The solving procedure is illustrated in Figure 5, and the inverse solving steps are described as follows.

Step 1. Establish PCS model and interval model to quantify the modeling parameters and the measured responses, respectively.

Step 2. Take the mean point of PCS model $\boldsymbol{U}^{\mathrm{M}}$ as the decomposition midpoint $\boldsymbol{U}^{\mathrm{C}}$, and assign the marginal CPs $\boldsymbol{U}_{-i}^{l_k}$.

Step 3. Construct the optimization matching model at marginal CP according to Eq. (15).

Step 4. Expand the performance function according to Eqs. (16) and (17).

Step 5. Establish the polynomial-based response surface model of each sub function according Eq. (18).

Step 6. Calculate the response intervals of each sub function by using affine algorithm according to Eq. (22).

Step 7. Calculate the response intervals of the forward function according to Eq. (16).

Step 8. Inverse the interval of unknown parameters combing GA and steps 4–7.

Step 9. Calculate the intervals of unknown parameters at all joint CPs according to Eq. (13).

Step 10. Obtain the intervals of unknown parameters $\boldsymbol{X}$ by comparing the all inverse intervals corresponding to the CPs in the PCS model.

4 Examples and Discussions

In this Section, the effectiveness of the proposed uncertain inverse method will be verified via two examples. In addition, the uncertain inverse results will be propagated forward, and the accuracy of the proposed uncertain inverse method can be verified by comparing the uncertain responses after propagation and the measured responses.

4.1 Load Identification of Plane Truss

The 25 bar plane truss shown in Figure 6 is employed to illustrate the validity of the proposed uncertain inverse method. The horizontal span of truss is 91.44 m, the vertical height is 15.24 m. The length L of each horizontal and vertical bar is 15.24 m. The joint node 12 is hinge-supported, and the joint nodes 6, 8 and 10 are roller-supported. The node 3 and node 5 are subjected to the vertical loads F_1 and one horizontal load F_2, respectively. The density and Poisson's ratio of bar are 7800 kg/m^3 and 0.3. Theoretically, the elastic modulus E and the cross-sectional areas A of bars are 200 GPa and 0.0052 m^2, respectively. Considering the uncertainty of the material and manufacturing process, the elastic modulus and cross-sectional area of some bars, there is a certain correlation between these uncertain parameters. Table 1 listed the number of bars and the left and right boundary of uncertain variables, and Table 2 showed the uncertain samples of elastic modulus and cross sectional area. Now, the vertical displacement intervals of node 3 and node 7 are measured by experiments, which are δ_3=[27.31, 36, 17] mm, δ_7=[54.19, 83.08] mm, and the loads F_1 and F_2 will be identified by the proposed uncertain inverse method.

The forward model for laid identification is expressed as

$$\begin{cases} \delta_3 = G_1(E_1, E_2, A_1, A_2, A_3), \\ \delta_7 = G_2(E_1, E_2, A_1, A_2, A_3). \end{cases} \tag{23}$$

Firstly, the PCS model is constructed according to the samples information to quantify the uncertain model variables. Through the PCA analysis, the PCA-based interval model is constructed. By combing the traditional

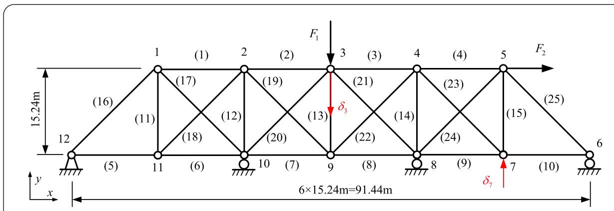

Figure 6 The 25-bar truss structure

Table 1 The information of uncertain variables

Uncertain variables	Number of bar	The interval
E_1 (GPa)	12, 17, 20	[172, 220]
E_2 (GPa)	14, 22, 23	[190, 242]
A_1 (10^{-5} m^2)	1, 11, 19	[474, 520]
A_2 (10^{-5} m^2)	10, 15, 25	[504, 546]
A_3 (10^{-5} m^2)	2, 3, 4	[530, 570]

Table 2 The uncertain samples of elastic modulus and cross-sectional areas

No.	E_1	E_2	A_1	A_2	A_3
1	193.55	199.94	483.69	516.33	557.19
2	180.20	205.09	475.50	533.20	530.00
3	197.44	219.59	484.36	524.87	545.63
4	185.93	200.91	493.09	524.45	540.06
5	195.43	222.24	490.09	519.66	541.48
6	197.20	211.34	494.25	526.65	560.05
7	210.37	223.13	491.70	515.63	542.36
8	215.95	242.00	513.15	504.00	550.91
9	195.36	231.73	492.17	518.38	557.84
10	180.55	205.90	476.72	532.07	533.98
11	203.96	198.57	493.66	528.92	567.00
12	208.51	237.36	503.16	514.38	537.26
13	192.59	212.59	502.65	524.18	567.19
14	185.45	198.39	479.16	522.05	557.93
15	184.61	190.24	483.89	540.25	541.96
16	193.30	205.52	489.60	516.30	563.46
17	194.00	234.50	503.49	504.11	558.13
18	190.11	203.12	509.57	522.80	543.14
19	195.75	227.85	487.32	531.32	533.62
20	197.78	209.24	515.79	511.90	568.59
21	176.39	190.35	483.45	540.92	538.05
22	220.00	230.36	520.00	520.71	533.50
23	172.00	200.96	474.00	522.36	546.00
24	195.65	221.52	493.44	521.94	551.84
25	187.48	225.78	509.64	515.95	556.02
26	196.23	207.20	492.63	527.90	531.04
27	193.90	190.00	487.14	546.00	564.30
28	178.17	230.40	481.18	507.68	533.72
29	198.36	195.18	502.02	535.06	551.27
30	198.48	210.07	483.88	521.69	543.34
31	195.01	219.09	486.01	532.02	539.27
32	208.32	203.44	501.86	533.46	558.00
33	200.77	208.20	508.35	517.63	555.15
34	199.62	213.70	495.37	529.31	570.00
35	183.58	205.11	496.05	514.84	549.93

interval and PCA-based interval model, the PCS model is established, which can be expressed as Eq. (24).

$$\Omega_P = \left\{ \boldsymbol{U} | \boldsymbol{U}^L \leq \boldsymbol{U} \leq \boldsymbol{U}^R \cap \boldsymbol{Z}^L \leq \boldsymbol{P}^T \left(\boldsymbol{U} - \boldsymbol{U}^M \right) \leq \boldsymbol{Z}^R \right\}, \tag{24}$$

where $\boldsymbol{U}$=[E_1, E_2, A_1, A_2, A_3]^T, and the mean point of the established PCS is $\boldsymbol{U}^M$=[194.3425, 212,3031, 493.6670, 523.3977, 549.1200]^T.

The four boundary vectors are

$$\begin{cases} \boldsymbol{U}^L = \begin{bmatrix} 172 \\ 190 \\ 474 \\ 504 \\ 530 \end{bmatrix}, \\ \boldsymbol{U}^R = \begin{bmatrix} 220 \\ 242 \\ 520 \\ 546 \\ 570 \end{bmatrix}, \\ \boldsymbol{Z}^L = \begin{bmatrix} -34.6828 \\ -29.9390 \\ -25.5109 \\ 10.8113 \\ -11.4418 \end{bmatrix}, \\ \boldsymbol{Z}^R = \begin{bmatrix} 45.7263 \\ 24.3515 \\ 17.2425 \\ 17.5878 \\ 10.8179 \end{bmatrix}. \end{cases} \tag{25}$$

The eigenvector matrix is

$$\boldsymbol{P}^T = \begin{bmatrix} 0.4233\,0.6588\,0.4776\, -0.3896\,0.0830 \\ 0.2181\, -0.4512\,0.3801\,0.1041\,0.7704 \\ -0.5365\,0.2042\, -0.3379\, -0.5429\,0.5115 \\ -0.4890\, -0.3254\,0.6517\, -0.3520\, -0.3261 \\ -0.4963\,0.4635\,0.2975\,0.6471\,0.1778 \end{bmatrix}. \tag{26}$$

In view of that, the proposed space collocation method is adopted to decouple the IP-MUS. The inverse function can be expressed as Eq. (27).

$$\overleftarrow{\boldsymbol{G}}(\boldsymbol{U}, \delta_3, \delta_7) \simeq \sum_{i=1}^{5} \overleftarrow{\boldsymbol{G}} \left(\boldsymbol{U}_{-i}^M, \delta_3, \delta_7 \right) - 4 \overleftarrow{\boldsymbol{G}} \left(\boldsymbol{U}^M, \delta_3, \delta_7 \right). \tag{27}$$

For each sub inverse function, 9 marginal CPs are taken. Thus, this complex IP-MUS is transformed into 41 IP-RU. For each IP-RU, the interval inverse method based on DRD and affine algorithm is adopted to inverse the intervals of unknown parameters $\boldsymbol{X}$. Firstly, the forward function is reconstructed by HDMR, and the each univariate sub function about $\boldsymbol{X}$ is further approximated by using the polynomial-based surrogate model. Because of the explicit expression of the surrogate model, the affine algorithm is employed to realize the interval propagation. Under these circumstances, the IP-RU with respect to each marginal CP is effectively solved. According to the inverse intervals of unknown parameters $\boldsymbol{X}$ at 45 marginal CPs, the intervals at all joint CPs (9^5 =59049) can be obtained using Eq. (27). It is found through calculation that there are 13008 CPs in the PCS model. Finally, the interval of unknown parameters $\boldsymbol{X}$ can be effectively obtained by comparing the all inverse intervals corresponding to these CPs in the PCS model, the corresponding inverse intervals are F_1=[2092.6867, 2726.4576] kN and F_1=[1375.7688, 2238.2330] kN.

In order to illustrate the accuracy of the proposed uncertain inverse method, the inversed intervals of uncertain parameters and PCS model of model variables are brought into the system model, and the forward propagation calculation is conducted by MCS. The intervals of calculated responses and measured responses are listed in Table 3. It can be found from Table 3 that the calculation interval is consistent with the measured interval. The maximum errors of left and right boundaries are 1.05% and 1.43%, respectively. These results represent that the proposed uncertain inverse method is effective and powerful for IP-MRU, which only highly improve the inverse efficiency, but also accurately identify the intervals of unknown loads.

4.2 Parameter Identification of Bimetal Beam

In the service process of mechanical equipment, due to the heat generated inside the structure and the change of working external environment temperature, the mechanical component and structure are subjected to thermal load, and then the structure thermal deformation and thermal stress are caused. Therefore, it is necessary to conduct thermo-mechanical coupling analysis of structure. During the thermo-mechanical coupling analysis, the thermal expansion coefficient is a key model parameter, which reflects the tendency of material to change its shape and density in response to a change in temperature. The larger the thermal expansion coefficient is, the greater the shape change of structure is affected by temperature. Therefore, it is of great significance to obtain the effective thermal expansion coefficient for structural reliability analysis and design.

Table 3 Interval comparison of the calculated and measured responses

	Calculated responses	Measured responses	Error
δ_3	[27.2484, 36.5655]	[27.3100, 36.1700]	[0.23%, 1.09%]
δ_7	[53.6210, 84.2714]	[54.1900, 83.0800]	[1.05%, 1.43%]

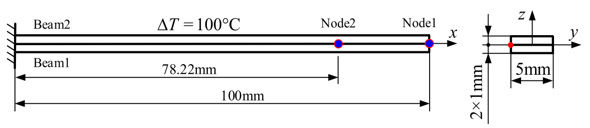

Figure 7 The structure of bimetallic beam

In this example, a coupled thermo-elasticity problem of bimetallic beam bonded by two materials is considering. The structure model of bimetallic beam is shown in Figure 7. Due to the different thermal expansion coefficient, the thermal deformations of the upper and lower beams are different, which will lead to the deflection deformation of bimetallic beam. Now, the thermal expansion coefficients of the upper and lower beams will be identified according to the deformations at two nodes as shown in Figure 7. For this bimetallic beam model, the initial temperature of bimetallic beam is 25 ℃, and the temperature rises to 125 ℃. The displacements of node 1 and node 2 in Z direction are measured, which are $\overline{\delta}_1^{\mathrm{I}}$= [6.2596, 8.7268] mm and $\overline{\delta}_2^{\mathrm{I}}$= [3.8426, 5.3574] mm, respectively. The forward model for parameter identification is expressed as

$$\begin{cases} \delta_1 = G_1(\alpha_1, \alpha_2, E_1, E_2), \\ \delta_2 = G_2(\alpha_1, \alpha_2, E_1, E_2), \end{cases} \tag{28}$$

where δ_1 and δ_2 are the displacement responses at node 1 and node 2, which are obtained by the finite element model. Considering that the material properties are affected by temperature, the sum of elastic modulus of two metal beams E_1 and E_2 are regarded as the uncertain variables, and the corresponding samples are shown in Table 4. α_1 and α_2 are the unknown thermal expansion coefficients that need to be inversed.

The proposed uncertain inverse method is used to realize the uncertainty identification of thermal expansion coefficients. Firstly, the PCS is established according to the samples provided in Table 3, the analytic expression of PCS model is

$$\Omega_{\mathrm{P}} = \left\{ \boldsymbol{E} \middle| \boldsymbol{E}^{\mathrm{L}} \le \boldsymbol{E} \le \boldsymbol{E}^{\mathrm{R}} \cap \boldsymbol{Z}^{\mathrm{L}} \le \boldsymbol{P}^{\mathrm{T}} \left(\boldsymbol{E} - \boldsymbol{E}^{\mathrm{M}} \right) \le \boldsymbol{Z}^{\mathrm{R}} \right\}, \tag{29}$$

where the eigenvector matrix $\boldsymbol{P}^{\mathrm{T}} = \begin{bmatrix} 0.6734 & 0.7393 \\ -0.7393 & 0.6734 \end{bmatrix}$, the mean point of PCS model $\boldsymbol{E}^{\mathrm{M}} = \begin{bmatrix} 137.1800 \\ 129.9567 \end{bmatrix}$, the boundaries $\boldsymbol{E}^{\mathrm{L}} = \begin{bmatrix} 127 \\ 120 \end{bmatrix}$, $\boldsymbol{E}^{\mathrm{R}} = \begin{bmatrix} 147 \\ 140 \end{bmatrix}$, $\boldsymbol{Z}^{\mathrm{R}} = \begin{bmatrix} -9.8993 \\ -5.8835 \end{bmatrix}$, and $\boldsymbol{Z}^{\mathrm{R}} = \begin{bmatrix} 9.5170 \\ 5.9836 \end{bmatrix}$.

Afterwards, the space collocation method based on DRD is adopted to decouple the IP-MRU, in which 7 marginal CPs are arranged on two expansion axis. At each marginal CP, the corresponding IP-RU is effectively solved by the proposed interval inverse method based on HDMR and affine algorithm. Finally, the intervals at all joint CPs are obtained using the inverse results at marginal CPs. The established PCS model and all CPs are shown in Figure 8. The intervals of thermal expansion coefficients α_1 and α_2 are effectively obtained by comparing the all inverse results corresponding to the CPs in the PCS model. The inversed thermal expansion coefficients are α_1^I= [17.9979, 24.1330] 10^{-6}/℃ and α_2^I = [3.8053, 5.4069]10^{-6}/℃.

It can be found from the above inverse results that the thermal expansion coefficient α_1 is much larger than α_2, thus the deformation of beam 1 is larger than that of beam 2 under the same temperature rise. However, because the two beams are bonded together, the deformation of beam 1 is restrained. In view of that, the whole metal beam produces the upward deflection deformation. Figure 9 shows the deflection deformation of bimetallic beam under different thermal expansion coefficients and elastic modulus. In order to further verify the effectiveness of the proposed uncertain inverse method,

Table 4 The samples of elastic modulus for two metal beams

No.	E_1 (GPa)	E_2 (GPa)	No.	E_1 (GPa)	E_2 (GPa)
1	127.00	127.67	11	131.40	124.40
2	147.00	132.00	12	131.80	121.47
3	131.00	127.33	13	134.60	120.00
4	135.00	129.33	14	135.40	128.40
5	139.00	134.67	15	137.00	130.00
6	143.00	131.00	16	138.20	124.53
7	136.20	127.87	17	139.40	140.00
8	133.00	127.00	18	143.80	136.80
9	138.20	136.33	19	141.40	135.33
10	138.60	130.00	20	142.60	135.00

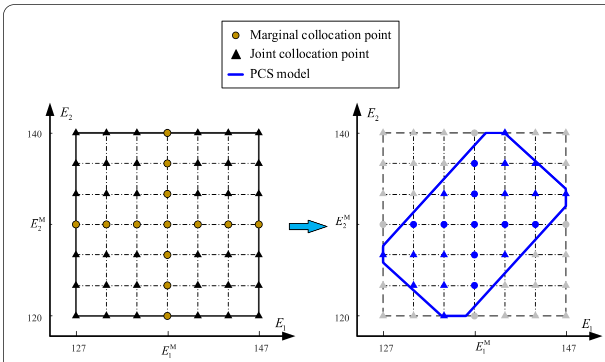

Figure 8 The CPs for solving IP-MRU

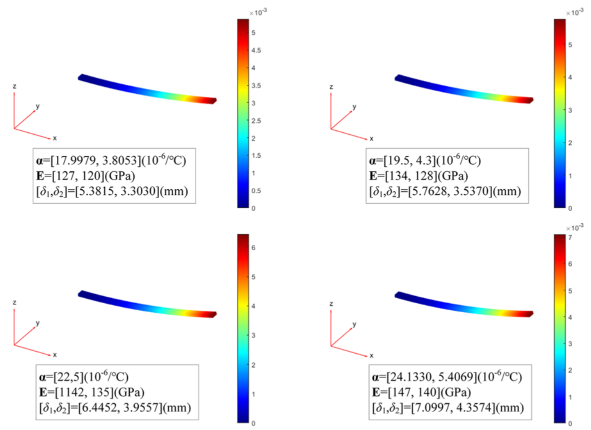

Figure 9 The deflection deformation of bimetallic beam under different structural parameters

Table 5 Interval comparison of nodes 1 and 2

	Calculated responses	Measured responses	Error
δ_1	[6.1989, 8.8074]	[6.2596, 8.7268]	[0.9706%, 0.9247%]
δ_2	[3.8053, 5.4069]	[3.8426, 5.3574]	[0.9695%, 0.9236%]

the inverse results are substituted into the forward model for propagation analysis. The calculated responses intervals and measured responses interval are compared in Table 4. It can be found from Table 5 that the errors of left and right boundaries at node 1 are [0.9706%, 0.9247%], the errors of left and right boundaries at node 2 are [0.9695%, 0.9236%]. These comparison results illustrate that the effectiveness of the proposed uncertain inverse method, and the inverse results can provide reliable and effective guidance for structural optimization design.

5 Conclusions

In practical engineering inverse problems, uncertainties often exist in the model itself and the measured responses at the same time. The solving of IP-MRU involves the complex multi-layer nesting because of the coupling of these multi-source uncertainties. In view of that, an efficient uncertain inverse method based on convex model and DRD is proposed to realize the interval identification of unknown structural parameters in this paper.

In proposed method, PCS model can flexibly quantify the epistemic uncertainty of modeling variables with irregular boundaries. Compared with the traditional interval model, PCS model provides the more compact uncertainty domain, and reasonably characterizes the correlation between uncertain variables. The space collocation method based DRD realizes the efficient decoupling of the IP-MRU. Through DRD for uncertain modeling variables, the IP-MRU are transformed into a few IP-RU at marginal CPs. Compared with MCS, the collocation method avoids a large number radon sampling, which effectively improves the solving efficiency of IP-RU and reduces the inverse computational cost. Furthermore, the interval inverse method based on HDMR and affine algorithm is proposed to realize the efficient solving of IP-RU. This method establishes the explicit surrogate model of the forward function by using HDMR and the polynomial-based response surface, and affine algorithm effectively improves the solving efficiency of IP-RU. The analysis results of two examples all indicate that the proposed uncertain inverse method provides an effective solving approach for IP-MRU, which can effectively identify the intervals of unknown structural parameters according to the uncertain measured responses and system model.

Acknowledgements

Not applicable.

Author contributions

JL and LC were in charge of the whole manuscript. LC supervised the project and wrote the manuscript. JL provided the funding acquisition and revised the manuscript. CL and WW assisted with simulation calculation and experimental analyses. All authors read and approved the final manuscript.

Authors' information

Lixiong Cao, born in 1986, is currently a postdocs at *Hunan University, China*. He received his PhD degree from *Hunan University, China*, in 2019. His research interests include uncertainty quantification, inverse problem theory and method, structural reliability analysis and optimization design, evidence theory.
E-mail: clx_328@hnu.edu.cn
Jie Liu, born in 1979, is currently a professor at *Hunan University, China*. He received his PhD degree from *Hunan University, China*, in 2011. His research interests include advanced design theory, engineering inverse problem theory and method, structural reliability analysis and optimization design, uncertainty quantification.
E-mail: liujie@hnu.edu.cn
Cheng Lu, born in 1987, is currently a Ph.D. candidate at *State Key Laboratory of Advanced Design and Manufacturing for Vehicle Body, College of Mechanical and Vehicle Engineering, Hunan University, China*. His research interests include optimization design, reliability analysis.
E-mail: lucheng@hnu.edu.cn
Wei Wang, born in 1978, is currently a Ph.D. candidate at *State Key Laboratory of Advanced Design and Manufacturing for Vehicle Body, College of Mechanical and Vehicle Engineering, Hunan University, China*. His research interests include optimization design of vehicle structure, reliability analysis.
E-mail: wangwei@csrzic.com

Funding

Supported by National Science Foundation of China (Grant No. 51975199), the Changsha Municipal Natural Science Foundation (Grant No. kq2014050).

Competing interests

The authors declare no competing financial interests.

Received: 15 August 2021 Revised: 23 May 2022 Accepted: 25 May 2022
Published online: 17 June 2022

References

[1] X Han, J Liu. *Numerical simulation-based design theory and methods*. Singapore: Springer Press, 2020.
[2] G R Liu, X Han. *Computational inverse techniques in nondestructive evaluation*. CRC Press, 2003.
[3] B Marchand, L Chamoin, C Rey. Parameter identification and model updating in the context of nonlinear mechanical behaviors using a unified formulation of the modified constitutive relation error concept. *Computer Methods in Applied Mechanics and Engineering*, 2019, 345: 1094-1113.
[4] N Grip, N Sabourova, Y M Tu. Sensitivity-based model updating for structural damage identification using total variation regularization. *Mechanical Systems and Signal Processing,* 2017, 84: 365-383.
[5] S Bureerat, N Pholdee. Inverse problem based differential evolution for efficient structural health monitoring of trusses. *Applied Soft Computing*, 2018, 66: 462-472.
[6] J Liu, K Li. Sparse identification of time-space coupled distributed dynamic load. *Mechanical Systems and Signal Processing*, 2021, 148: 107177.
[7] Y J Luo, Z Kang, A Li. Structural reliability assessment based on probability and convex set mixed model. *Computers & Structures*, 2009, 87: 1408-1415.
[8] X Wu, T Mui, G J Hu, et al. Inverse uncertainty quantification of TRACE physical model parameters using sparse gird stochastic collocation surrogate model. *Nuclear Engineering and Design*, 2017, 319: 185-200.
[9] G Roma, F D Maio, A Bersano, et al. A Bayesian framework of inverse uncertainty quantification with principal component analysis and Kriging for the reliability analysis of passive safety systems. *Nuclear Engineering and Design*, 2021, 379: 111230.
[10] B Huang, X P Du. Probabilistic uncertainty analysis by mean-value first order saddlepoint approximation. *Reliability Engineering & System Safety*. 2008, 93: 325-336.
[11] J Mcfarland, E Decarlo. A Monte Carlo framework for probabilistic analysis and variance decomposition with distribution parameter uncertainty. *Reliability Engineering & System Safety*, 2020, 197: 106807.
[12] A Tarantola. Popper, Bayes and the inverse problem. *Nature Physics*, 2006, 2(8): 492-494.
[13] Z D Xu, Y H Cao, M Zhao. Parameter identification of tailplane iced aircraft based on maximum likelihood method. *Applied Mechanics & Materials*. 2012, 192: 57-62.
[14] J M Nichols, W A Link, K D Murphy, et al. A Bayesian approach to identifying structural nonlinearity using free-decay response: Application to damage detection in composites. *Journal of Sound and Vibration*, 2010, 329: 2995-3007.
[15] J Liu, X H Meng, C Xu, et al. Forward and inverse structural uncertainty propagations under stochastic variables with arbitrary probability distributions. *Computer Methods in Applied Mechanics and Engineering*, 2018, 342: 287-320.
[16] V H Hoang, C Schwab, A M Stuart. Complexity analysis of accelerated MCMC methods for bayesian inversion. *Inverse Problems*, 2012, 29: 317-322.
[17] G Hu, T Kozlowski. Inverse uncertainty quantification of trace physical model parameters using BFBT benchmark data. *Annals of Nuclear Energy*, 2016, 96: 197-203.
[18] L X Cao, J Liu, C Xu, C Lu, X B Bu. Uncertain inverse method by the sequential FOSM and its application on uncertainty reconstruction of vehicle–pedestrian collision accident. *International Journal of Mechanics and Materials in Design*, 2021, 17: 41-54.
[19] X P Du. Inverse simulation under uncertainty by optimization. *Journal of Computing and Information Science in Engineering*, 2013, 13: 021005.
[20] J Liu, Y F Hu, C Xu, et al. Probability assessments of identified parameters for stochastic structures using point estimation method. *Reliability Engineering & System Safety*, 2016, 156: 51-58.
[21] X H Meng, J Liu, L X Cao, et al. A general frame for uncertainty propagation under multimodally distributed random variables. *Computer Methods in Applied Mechanics and Engineering*, 2020, 367: 113109.
[22] H P Wan, W X Ren, M Todd. An efficient metamodeling approach for uncertainty quantification of complex systems with arbitrary parameter probability distributions. *International Journal for Numerical Methods in Engineering*, 2017, 109: 739-760.
[23] G Wei, C Song, F Tin-Loi. Probabilistic interval analysis for structures with uncertainty. *Structural Safety*, 2010, 32: 191-199.
[24] J C Helton, J D Johnson, W L Oberkampf, et al. A sampling-based computational strategy for the representation of epistemic uncertainty in model predictions with evidence theory. *Computer Methods in Applied Mechanics and Engineering*, 2007, 196: 3980-3998.
[25] J J Zhu, Z P Qiu. Interval analysis for uncertain aerodynamic loads with uncertain-but-bounded parameters. *Journal of Fluids and Structures*, 2018, 81: 418-436.
[26] I Elishakoff, P Elisseeff, S A L Glegg. Nonprobabilistic, convex-theoretic modeling of scatter in material properties. *AIAA Journal*, 2012, 32: 843-849.
[27] J Liu, L X Cao, C Jiang, et al. Parallelotope-formed evidence theory model for quantifying uncertainties with correlation. *Applied Mathematical Modelling*, 2020, 77: 32-48.
[28] L X Cao, J Liu, L Xie, et al. Non-probabilistic polygonal convex set model for structural uncertainty quantification. *Applied Mathematical Modelling*, 2021, 89: 504-518.
[29] M Faes, M Broggi, E Patelli, et al. A multivariate interval approach for inverse uncertainty quantification with limited experimental data. *Mechanical Systems and Signal Processing*, 2019, 118: 534-548.
[30] C Jiang, G R Liu, X Han. A novel method for uncertainty inverse problems and application to material characterization of composites. *Experimental Mechanics*, 2008, 48: 539-548.
[31] J Liu, X Sun, X Han, et al. Dynamic load identification for stochastic structures based on Gegenbauer polynomial approximation and regularization method. *Mechanical Systems and Signal Processing*, 2015, 56-57: 35-54.
[32] M H Xu, N Jiang. Dynamic load identification for interval structures under a presupposition of 'being included prior to being measured'. *Applied Mathematical Modelling*, 2020, 85: 107-123.
[33] D Wei, S Rahman. Structural reliability analysis by univariate decomposition and numerical integration. *Probabilistic Engineering Mechanics*, 2007, 22: 27-38.
[34] L X Cao, J Liu, C Jiang, et al. Evidence-based structural uncertainty quantification by dimension reduction decomposition and marginal interval analysis. *Journal of Mechanical Design*, 2019, 142: 1-36.
[35] J Liu, H Cai, C Jiang, et al. An interval inverse method based on high dimensional model representation and affine arithmetic. *Applied Mathematical Modelling*, 2018, 63: 732-743.